ORIGINAL ARTICLE

Combined use of phospholipid complexes and self-emulsifying microemulsions for improving the oral absorption of a BCS class IV compound, baicalin

Huiyi Wu[a], Xiaoying Long[a],*, Fei Yuan[a], Li Chen[a], Sujing Pan[a], Yunjun Liu[a], Yoshiko Stowell[b], Xiaoling Li[b]

[a]*School of Traditional Chinese Medicine, Guangdong Pharmaceutical University, Guangzhou 510006, China*
[b]*Department of Pharmaceutics, Thomas J Long School of Pharmacy & Health Sciences, University of the Pacific, CA 95211, USA*

Abstract The aim of this study was to develop a formulation to improve the oral absorption of baicalin (BA) by combining a phospholipid complex (PC) and self-emulsifying microemulsion drug delivery system (SMEDDS), termed BA–PC–SMEDDS. BA–PC was prepared by a solvent evaporation method and evaluated by complexation percentage (CP). The physicochemical properties of BA–PC were determined. The synergistic effect of PC and SMEDDS on permeation of BA was studied *in vitro* with Caco-2 cells and *in situ* with a single pass intestinal perfusion model. The improved bioavailability of BA in BA–PC–SMEDDS was confirmed in an *in vivo* rat model. The CP of BA–PC reached 100% when the molar ratio of drug to phospholipid (PP) was $\geq$ 1:1. The solubility of BA–PC increased in both water and octanol, and the log $P_{o/w}$ of BA–PC was increased significantly. BA–PC–SMEDDS could be dispersed more evenly in water, compared to BA and BA–PC. Both the Caco-2 cell uptake and single-pass intestinal perfusion models illustrated that transport of BA in BA–PC was lower than that of free BA, while

---

*Corresponding author. Tel.: +86 20 39352559.
    E-mail address: longxy3156@163.com (Xiaoying Long).

Production and hosting by Elsevier

improved significantly in BA–PC–SMEDDS. The relative bioavailability of BA–PC(1:2)–SMEDDS was 220.37%. The combination system of PC and SMEDDS had a synergistic effect on improving the oral absorption of BA.

1. Introduction

Baicalin (BA, 5,6-dihydroxy-4-oxygen-2-phenyl-4*H*-1-benzopyran-7-β-D-glucopyranoseacid), as shown in Fig. 1, is a major flavonoid component extracted from the rhizomes of the traditional Chinese medicinal herb *Scutellaria baicalensis* Georgi. BA has been reported to possess a wide range of pharmacological and biological effects including anti-inflammatory[1,2], anti-endotoxin[3], anti-allergic[4], antimicrobial[5], antioxidant[6,7], antiproliferative[8,9] and anti-tumor[10,11] actions. The clinical applications of BA include the treatment of pneumonia, hepatitis, cardiovascular diseases and cancer[11–13]. Because of low oral bioavailability[14], various formulations have been developed to improve the gastrointestinal (GI) absorption of BA. Solid dispersions[15], microcapsules[16,17], cyclodextrins[18], emulsions[19], phospholipid complex[20], liposomes[21] and nanoparticles[22] have been described. Based on the extremely low hydrophilicity (solubility 0.052 mg/mL in water) and lipophilicity ($P_{app}=0.037 \times 10^{-6}$ cm/s), BA may be classified as a class IV compound according to Biopharmaceutical Classification System (BCS).

Recently, complexes of phospholipid with various poorly absorbed compounds have been explored to improve the bioavailability of orally administered drugs. Phospholipid complex (PC) is obtained by the interaction of natural or synthetic phospholipids (PP), such as phosphatidylcholine, phosphatidylethanolamine or phosphatidyiserine with the selected botanical derivatives at an appropriate ratio in an aprotic solvent[23]. Since PP is a component of biological membranes[24] and can alter the hydrophobicity of a drug after formation of the PC, it is hypothesized that the formation of a drug-PC could increase the permeation of drugs across membranes. Previous studies suggested that the oral bioavailability of poorly absorbed phytoconstituents can be improved by using PC drug delivery systems[25–27]. Although PC may significantly increase membrane transport, the higher lipophilicity of PC led to a poorer dispersion in aqueous media including GI fluid, as determined in a preliminary study by our group.
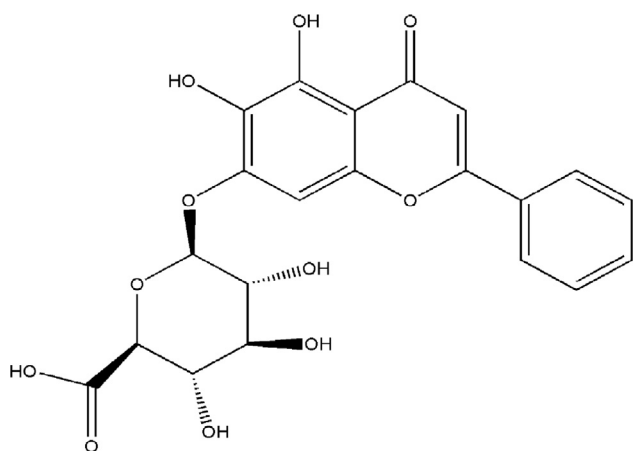
When the size of oil droplets is reduced to a nanometer scale, formulating a low aqueous solubility drug into an emulsion dosage form is an effective method to increase the surface area of the dispersed phase that contains poorly water soluble drugs. Self-emulsifying microemulsion (SMEDDS, size of oil droplets <500 nm) can be formed with a low-energy requirement under such conditions as gentle agitation or even gastric mobility[28–30]. SMEDDS can enhance drug absorption *via* improved dissolution and diffusion, facilitated intestinal lymphatic transport of drugs, protection against enzymatic hydrolysis[31] and inhibition of efflux by P-glycoprotein (P-gp)[32]. This method has been shown to be effective for BCS II drugs, *e.g*., silymarin, oridonin and curcumin[33–35]. Although SMEDDS has been reported to increase the bioavailability of many drugs by increasing water solubility, the increase in bioavailability of BCS IV compounds using SMEDDS is limited.

The objectives of this study were to design a delivery system that will take advantage of both PC and SMEDDS to improve the absorption of BA in the GI and probe the mechanisms of bioavailability enhancement by characterizing the solubility and partition coefficients as well as investigating the change in lipophilicity after formation of PC. *In vitro* cell permeation, *in situ* single-pass intestinal perfusion (SPIP) and *in vivo* bioavailability studies were conducted to demonstrate the effect of the BA–PC–SMEDDS system on bioavailability enhancement.

2. Materials and methods

2.1. Materials and animals

Baicalin was purchased from Xi'an Xiaocao Plant Technology Co., Ltd. (Xi'an, China; purity: 98%). Lipoid S75 was supplied by Shanghai Dongshang Biological Technology Co., Ltd. (Shanghai, China). Purified ovolecithin was obtained from Guangzhou HanFang Modern Traditional Chinese Medicine Research Co., Ltd. (Guangdong, China). Caco-2 cells were a generous gift from the Laboratory of Dr. Huang at the School of Pharmaceutical Sciences, Sun Yat-Sen University (Guangdong, China). Ethyl oleate and glycerol (molecular biology grade) were purchased from Aladdin Reagent Co., Ltd. (Shanghai, China). Tween-80 was supplied by Shanghai ShenYu Pharmaceutical and Chemical Industry Co., Ltd. (Shanghai, China). Tetrahydrofuran was purchased from Tianjin Zhiyuan Chemical Reagents Co., Ltd. (Tianjin, China). Methanol, *n*-octanol, isopropanol, anhydrous ethanol and potassium dihydrogen phosphate were purchased from Tianjin Damao Chemical Reagent Factory (Tianjin, China). Sodium hydroxide and concentrated hydrochloric acid were obtained from Tianjin Baishi Chemical Co., Ltd. (Tianjin, China). Hanks' Balanced Salt Solution (HBSS) solution was obtained from Hangzhou Gino Bio-pharmaceutical Technology Co., Ltd. (Zhejiang, China). High purity liquid nitrogen was purchased from Guangzhou Junduo Gas Co., Ltd. (Guangdong, China). Acetonitrile and methanol (HPLC grade) were purchased from Dikma

Figure 1 The chemical structure of BA.

Technologies Inc. (Beijing, China). All other chemicals and solvents used in this study were of analytical grade.

Sprague-Dawley rats weighing 200 ± 20 g were purchased from the Animal Center of Guangdong Medical Laboratory (Guangdong, China). The protocol for animal experiments was approved by the Guangdong Pharmaceutical University Experimental Animal Ethics Committee.

2.2. Preparation of BA–PC

BA–PC was prepared according to a previously published method[36] with modifications. Briefly, BA and PP at molar ratios of 1:0.5, 1:1, 1:1.5 and 1:2 were added in a 50 mL conical flask with tetrahydrofuran (1 mg of BA/0.2 mL) as solvent. The suspension was sonicated for 15 min and maintained at 45 °C with stirring in a water bath for 0.5 h to dissolve the drug and form the complex. Tetrahydrofuran was evaporated under vacuum at 40 °C using a rotary vacuum evaporator. The dried residues were placed in a sealed vial and kept at 4 °C. The molar ratio of BA and PP in the complexes was determined by complexation percentage (CP) of BA, using the following equation:

$$CP(\%) = \frac{a-b}{a} \times 100\% \qquad (1)$$

where a is the initial weight of BA, b is the weight of free BA in BA–PC. The weight of free BA in BA–PC was measured according to the difference of solubility among BA, BA–PC and PP in chloroform, i.e., both BA–PC and PP can dissolve in chloroform, but free BA was insoluble in chloroform. The precipitate of BA in chloroform was dissolved in methanol and analyzed by using a UV spectrophotometer at 316 nm.

2.3. Determination of solubility and apparent oil–water partition coefficient

The solubility of BA and BA–PC was determined by adding an excess of BA or BA–PC to a vial containing 5 mL of water or octanol. The vials were sealed and placed in a water bath shaker at 37 °C for 48 h with continuous shaking at 100 rpm. The suspensions were then filtered with 0.22 µm filter immediately at the same temperature to remove the insoluble substances. The concentrations of BA in the filtrate were determined by a UV spectrophotometry. Three replicate analyses were carried out for each formulation, and the data are presented as means $\pm$ SD.

The apparent oil–water partition coefficient ($P_{o/w}$) was obtained using the method described previously[37,38]. Solutions of BA or BA–PC (BA 50 µg/mL) were prepared in water-saturated octanol. These solutions were then equilibrated at 37 °C with an equal volume (5 mL) of octanol-saturated water using a magnetic stirrer at 700 rpm for 24 h. The phases were then separated by centrifugation. The total drug concentration in water-saturated octanol before equilibration and that in the octanol phase after separation, C_{total} and C_o, respectively, were determined using a UV spectrophotometer as described above. The concentration of drug in the aqueous phase, C_w, was obtained from the mass balance ($C_w = C_{total} - C_o$). Experiments were performed in triplicate to assess reproducibility and data were presented as means $\pm$ SD. $P_{o/w}$ was calculated using the following equation:

$$P_{o/w} = \frac{C_o}{C_w} \qquad (2)$$

where C_o is the concentration of BA in octanol and C_w is the concentration of BA in water.

2.4. Dispersible uniformity and stability of BA–PC and BA–PC–SMEDDS

For the current study, a pre-microemulsion concentrate (PMC) of SMEDDS developed previously in our lab was used. Ethyl oleate, Tween-80 and glycerol (weight ratio of 1:2.25:1.75) were mixed at ambient temperature and loaded with BA–PC (equivalent to 75 mg of BA) at different drug to PP molar ratio of 1:1, 1:1.5 or 1:2. The mixtures were heated at 65 °C in a water bath and stirred mildly to get PMC.

The microemulsion was formed spontaneously by adding PMC dropwise to 100 mL of distilled water in a wide-mouth bottle under gentle stirring for two minutes at 37 °C in a water bath. BA–PC was dispersed in water by sonication. Free BA was dispersed in water by a simple agitation. All samples were maintained at 37 °C in a water bath. The concentration of BA in the upper solution was determined at 316 nm by UV spectrophotometry at 0, 4, 8, 12 and 24 h.

2.5. Caco-2 cell permeation studies of BA, BA–PC and BA–PC–SMEDDS

Transepithelial permeation studies were performed using a previously described method[39–41]. The Caco-2 cells were cultured in Dulbecco's Modified Eagle Medium (DMEM) containing 4.5 mg/mL glucose, 10% FCS, 1% nonessential amino acids, 1% sodium pyruvate, 1% glutamine, and 1% penicillin/streptomycin under 5% CO_2 and 95% relative humidity at 37 °C. When the confluency reached 80% the cells were seeded at the density of 2×10^5 cells/cm^2 onto the membranes of Transwell inserts coated with type-I collagen (12-well Transwell plate, 0.4 mm pore size, 12 mm diameter, 1.12 cm^2 area, Corning Display Technologies (China) Co., Ltd.) and cultured for 21 days in DMEM. The medium was replaced every 48 h for the first 6 days and every 24 h thereafter. The integrity of the cell layer was evaluated by measuring the transepithelial electrical resistance (TEER) using Millicell-ERS (Millipore Corporation, Bedford, MA) before and after each transport experiment. Permeation studies were conducted when TEER value was greater than $250 \, \Omega \cdot cm^2$.

Prior to the permeation experiment, the media on both sides of transwell monolayers were replaced 3 times with HBSS and then equilibrated for 30 min. The medium of the apical-side was removed and replaced with 0.5 mL of the test solutions (pH 6.8, 37 °C) containing BA at different concentrations (375 µg/mL, 281.2 µg/mL and 187.5 µg/mL), BA–PC or BA–PC–SMEDDS at different drug to PP molar ratios of 1:1, 1:1.5 and 1:2 containing 187.5 µg/mL of BA. The basolateral side contained 1.5 mL of HBSS. The transport plates were kept at 37 °C in a shaking incubator at 50 rpm. Samples (100 µL) were taken from the basolateral side at 30, 60, 90, 120 and 180 min. An equal volume of the fresh HBSS was added following each sample withdrawal. The collected samples were centrifuged at 14,000 rpm for 10 min and the concentration of BA was analyzed by using an HPLC system (Waters 1525 HPLC pump, 2489 UV detector, Milford, USA) at 270 nm with a C18 column (Platisil, 250 mm × 4.6 mm, 5 µm). A mixture of acetonitrile and water (27:73) which contains 0.035% of triethylamine and 0.025% of phosphoric acid was used as a mobile phase. The flow rate was set at 1 mL/min.

Measurement of basolateral-to-apical transport was carried out by adding 0.5 mL of HBSS to the apical side and 1.5 mL of the test solutions to the basolateral side. Other procedures were performed as described in the apical to basolateral studies. Free BA solution (187.5 µg/mL) was prepared with HBSS containing 100 µg/mL of verapamil, a P-gp inhibitor, to study apical-to-basolateral and basolateral-to-apical transports using the same procedures. The cumulative permeation quantity (Q, µg), apparent permeability coefficients (P_{app}, cm/s) and efflux ratio (ER) were calculated using Eqs. (3)–(5), correspondingly.

$$Q = C_n V_1 + \sum_{m=1}^{n-1} C_m V_2 \qquad (3)$$

where C_n is the drug concentration in the receiver compartment at the nth time point (µg/mL), $\sum_{m=1}^{n-1} C_m$ represents the cumulative concentration from the first to the $(n-1)$th time point (µg/mL) which corrects for the withdrawn samples, and V_1 and V_2 correspond to the volumes of the receptor compartment and the collected samples at each time point (mL), respectively.

$$P_{app} = \frac{dQ}{dt} \times \frac{1}{AC_0} \qquad (4)$$

where dQ/dt is the steady-state flux (µg/min) of drug, which is obtained from the slope of the linear regression of cumulative transport amount *versus* time curve, C_0 is the initial concentration in donor chamber (µg/mL), and A is the surface area of the monolayer (cm^2).

$$ER = P_{app}(B-A)/P_{app}(A-B) \qquad (5)$$

where $P_{app}(B-A)$ is the permeability coefficient determined by the transport of drug from the basal to the apical compartment, and $P_{app}(A-B)$ is that from the apical to the basal direction.

Data are reported as means $\pm$ SD, $n=3$ for individual groups. The unpaired Student's t-test was used to determine statistical significance by using ANOVA of JMP$^{\circledR}$, version10.0.0 software (SAS Institute Inc., USA) and P values of less than 0.05 were considered significant.

2.6. Single-pass intestinal perfusion studies of BA, BA–PC and BA–PC–SMEDDS

Sprague-Dawley rats weighing 200 ± 20 g were used in the perfusion studies. Prior to the experiments, the animals were fasted overnight for at least 12 h with free access to water. The rats were randomly assigned to five experimental groups.

The procedure for the SPIP experiment was taken from the previous literature[42–45]. Rats were anaesthetized by an intraperitoneal injection of 6 mL/kg urethane (10% *w/v*) and placed on a plank and kept warm with a table lamp. The abdomen was opened using a longitudinal incision of 3–4 cm along the midline. After the small intestine was carefully exposed, a 10 cm segment of intestine (including duodenum and jejunum, ileum, and colon) was cannulated at both ends with flexible PVC tubing (2.29 cm, i.d.) and ligated using silk thread. The exposed segment was kept moist with 37 °C saline solution. Krebs–Ringer (KR) buffer was used as perfusate, which consisted of NaCl, 7.8 g/L; KCl, 0.35 g/L; CaCl$_2$, 0.37 g/L; NaH$_2$PO$_4$, 0.22 g/L; NaHCO$_3$, 1.37 g/L; MgCl$_2$, 0.22 g/L; and glucose, 1.4 g/L, and adjusted to pH 6.0 using phosphoric acid. Test solutions used in the perfusion study were prepared by dissolving BA, BA–PC or BA–PC–SMEDDS at drug to PP molar ratios of 1:1 and 1:2 in KR buffer at a 750 µg/mL final concentration of BA. The intestinal segments were gently rinsed

with a blank KR solution to remove intestinal contents. The test solution was infused by a circulation pump at a flow rate of 1.0 mL/min for 10 min followed by adjustment to 0.2 mL/min for 30 min to reach the steady-state condition. When the concentration ratio of phenol red ('non-absorbed' marker) between inlet and outlet approached one, the outflow perfusate was collected at a 15 min interval for 150 min. Concentrations of phenol red and BA were analyzed by the same HPLC method as described in Section 2.5. The length of the small intestine segment was measured after the final collection.

The absorption of water was corrected by phenol red concentration at inlet and outlet using[46].

$$C_{out(corrected)} = \frac{C_{out} C_{PR(in)}}{C_{PR(out)}} \qquad (6)$$

where C_{out} is the drug concentration measured in the outlet perfusate, $C_{PR(in)}$ and $C_{PR(out)}$ are the concentrations of phenol red at inlet and outlet, respectively. The effective permeability (P_{eff}) was calculated using

$$P_{eff} = \frac{Q \ln(C_{in}/C_{out(corrected)})}{2\pi RL} \qquad (7)$$

where C_{out}(corrected) is the corrected drug concentration in the outlet perfusate at the steady state, C_{in} is the drug concentration at the inlet, Q is the perfusion flow rate (0.2 mL/min), L is the length of intestinal segment (cm), and R is the radius of intestinal segment (cm). Statistical analysis was carried out as described in Section 2.5.

2.7. Oral bioavailability of BA–PC–SMEDDS and BA suspensions

Rats were fasted overnight for at least 12 h before dosing, with free access to water throughout the experiments. Twelve male and female Sprague-Dawley rats weighing 200 ± 20 g were divided randomly into two groups of six each with the equal number of male and female. The rats in each group were gavaged with 5 mL of BA or BA–PC(1:2)–SMEDDS dispersed in water, each containing 75 mg of BA. Under ether anesthesia, 0.3 mL of blood samples were collected through the orbital vein prior to dosing and at the predetermined time of 0.167, 0.5, 1.0, 1.5, 2.0, 3.0, 4.0, 6.0, 8.0 and 12.0 h post-dosing. The blood samples were collected in polypropylene tubes with heparin, and then centrifuged immediately at 3500 rpm for 15 min to obtain plasma. The plasma was mixed with 0.25 mL of 10% of perchloric acid–methanol solution and mixed for 3 min using a XW-80A vortex mixer to precipitate protein[47]. The suspension was centrifuged at 3500 rpm for 15 min and the supernatant was analyzed by HPLC with the same chromatographic conditions as described in Section 2.5 to determine the concentration of BA.

The biopharmaceutical and pharmacokinetic parameters, *i.e.*, maximum peak concentration (C_{max}), time to reach C_{max} (T_{max}), area under plasma time curve (AUC) were obtained by using WinNonlin, version 6.1 (Pharsight, A Certara$^{™}$ Company, USA), noncompartmental analysis. The relative bioavailability (F_r) was calculated using

$$F_r = \frac{AUC_T}{AUC_R} \times 100\% \qquad (8)$$

where AUC_T refers to the area under plasma time curve of test formulation and AUC_R refers to the area under plasma time curve of control. Experimental values are expressed as mean $\pm$ SD.

Unpaired *t*-test was performed by using ANOVA of JMP®, version 10.0.0 software (SAS Institute Inc., USA) and the data were considered statistically significant at $P < 0.01$.

3. Results and discussion

3.1. Complexation percentage, solubility and oil–water partition coefficient of BA–PC

At different drug to PP molar ratios, the CP (%), solubility and $P_{o/w}$ of BA and BA–PC in water and octanol are shown in Table 1. The CP (%) reached 100% when molar ratio of drug to PP was above 1:1. Though BA–PC increased the solubility of BA in water and octanol, the improvement of solubility in octanol was more significant than that in water. When the molar ratio of BA to PP was increased from 1:1 to 1:2, the solubility of BA–PC increased 48–85 times in octanol which made log $P_{o/w}$ increase from -1.03 to -0.105, -0.024 and 0.18, correspondingly, compared with BA.

It is generally known that most drugs cross the lipid-rich epithelial cells of the small intestine by passive diffusion and high solubility and high permeability are important for a high bioavailability. Thus, it is an effective method to increase bioavailability of BA by improving its water solubility and biofilm permeability. $P_{o/w}$ has been associated with the biomembrane permeability of drugs; drugs with a log $P_{o/w}$ in a range between -1 and 2[48] have been shown to have good oral absorption. When log $P_{o/w}$ is lower than -1 or higher than 2, drug absorption tends to be lower due to the poor permeability or poor partition between biomembrane and intracellular fluid. The data in Table 1 revealed that log $P_{o/w}$ of BA–PC at different BA to PP molar ratios was within the optimal range contrary to that of BA, and 1:2 was better than 1:1 and 1:1.5.

3.2. Dispersible uniformity and stability in water

Even though the high log $P_{o/w}$ of BA–PC may improve the permeability of BA, the data in Table 1 illustrated BA–PC increased the solubility of BA in water slightly and BA–PC could not be dispersed homogeneously in water (Fig. 2). When BA was dispersed in water, the concentration of BA in the upper solution was nearly zero initially (solid rhombus in Fig. 2). For BA–PC, the concentrations of BA decreased to 30%–60% of the original concentration at different molar ratios of BA to PP (1:1 (solid round), 1:1.5 (solid triangle) and 1:2 (solid square)) after 24 h at 37 °C. But the concentrations of BA remained above 80% of the original concentration for BA–PC–SMEDDS (1:1, 1:1.5, 1:2, opening shape in Fig. 2) with a particle size of about 228 nm

(Fig. 3). Visually, the precipitates of free BA and BA–PC at molar ratios of BA to PP 1:1 and 1:1.5 were found at the bottom of the bottles, but there was very little precipitate for BA–PC at molar ratio of BA to PP 1:2 and all BA–PC–SMEDDS. In water, BA possibly dissociated from BA–PC when the hydrogen bonding force between BA and water was greater than that between BA and
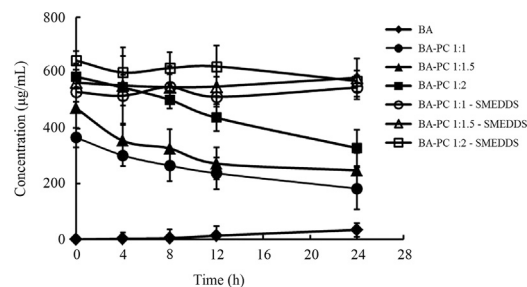

Figure 2 The concentration change of BA in the upper solution part of water over time when BA, BA–PC, BA–PC–SMEDDS were dispersed in water at 37 °C. Data are expressed as mean$\pm$SD ($n=3$).
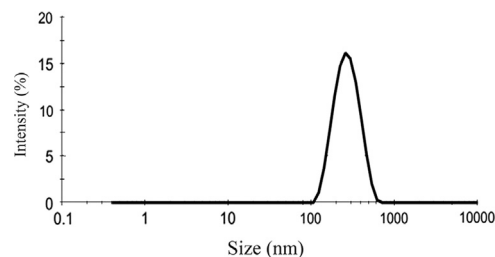

Figure 3 Particle size of BA–PC–SMEDDS.

Table 2 Apparent permeability coefficients (P_{app}) and efflux ratio (ER) of BA with or without verapamil.

Formulation	P_{app} ($\times 10^{-6}$, cm/s)[a]		ER
	AP–BL	BL–AP	
BA	0.119 ± 0.092	0.365 ± 0.096	3.067
BA+verapamil	0.622 ± 0.101*	0.174 ± 0.000*	0.280

[a]Data were expressed as mean$\pm$SD, $n=3$.
*$P < 0.05$ compared to BA.

Table 1 The complexation percentage (CP), solubility and apparent oil–water partition coefficient (log $P_{o/w}$) in various formulations.

Formulation	Molar ratio of BA to PP	CP (%)	Solubility of BA (mg/mL)[a]		log $P_{o/w}$ (37 °C)[a]
			Water	Octanol	
BA	—	N/A	0.052 ± 0.0015	0.136 ± 0.012	-1.032 ± 0.014
BA–PC	1:0.5	80	N/A	N/A	N/A
	1:1	100	0.092 ± 0.0066	6.542 ± 0.96*	-0.105 ± 0.005
	1:1.5	100	0.129 ± 0.0028	9.065 ± 0.76*	-0.024 ± 0.009
	1:2	100	0.157 ± 0.0003	11.68 ± 1.13*	0.182 ± 0.006

[a]Data were expressed as mean$\pm$SD, $n=3$.
*$P < 0.05$ compared to BA. N/A, no data available.

PP, leading to a decrease in the concentration of BA in the upper solution part and the formation of precipitates at low molar ratio of BA to PP. There were no precipitates for BA–PC at 1:2 M ratio of BA to PP because of the strong hydrogen bonding at a high molar ratio of BA to PP. However, the concentration decrease in BA in the upper solution was very limited for all BA–PC–SMEDDS. This may be attributed to the oil in SMEDDS which weakens the hydrogen bonding force between BA and water while surfactants can facilitate the dispersion of BA–PC. Therefore, the concentration reduction of BA in water may be related not only to the

nonuniform dispersion of BA–PC but also to the poor stability caused by the dissociation of BA from BA–PC.

3.3. In vitro permeation through Caco-2 cell model

As shown in Fig. 4a, Q was increased with an increase in the concentration of BA, and P_{app} was almost the same at corresponding concentrations ($P>0.05$) as shown in Fig. 4b. The data suggest the passive diffusion mechanism of BA transport. It is obvious from Table 2 that the presence of verapamil significantly increased the $A \rightarrow B$ permeation ($P<0.05$) and reduced the $B \rightarrow A$ efflux ($P<0.05$), causing a decrease in ER from 3.067 to 0.280. These results suggest that BA may be a substrate of P-gp which partly explains the low biomembrane permeability of BA and SMEDDS formulations containing Tween 80, a P-gp inhibitor, to decrease efflux of P-gp[49,50].

The transcellular transport of BA–PC and BA–PC–SMEEDS across the Caco-2 monolayer compared with that of free BA is shown in Fig. 5 and Table 3. The Q and P_{app} of BA–PC were lower than that of free BA and decreased following the increase in the molar ratio of BA to PP (Fig. 5a and Table 3), though the P_{app} at 1:1 M ratio of BA to PP was a little higher than that of BA. In theory, PC could promote the biomembrane permeation of BA by high log $P_{o/w}$, and the reason why the Q of BA–PC was lower than that of free BA could be explained from the data in Table 1 and Fig. 2. PC increased the solubility of BA in water only 1.7-fold but

Table 3   Apparent permeability coefficients (P_{app}) through Caco-2 monolayer of BA, BA–PC and BA–PC–SMEDDS at various molar ratios of drug to PP.

Formulation	P_{app} ($\times 10^{-6}$, cm/s)
BA	0.037 ± 0.012
BA–PC(1:1)	0.045 ± 0.012
BA–PC(1:1.5)	0.024 ± 0.008
BA–PC(1:2)	0.017 ± 0.002[*]
BA–PC(1:1)–SMEDDS	0.328 ± 0.036[*]
BA–PC(1:1.5)–SMEDDS	0.690 ± 0.057[*]
BA–PC(1:2)–SMEDDS	0.774 ± 0.084[*]

Data were expressed as mean$\pm$SD, $n=3$.
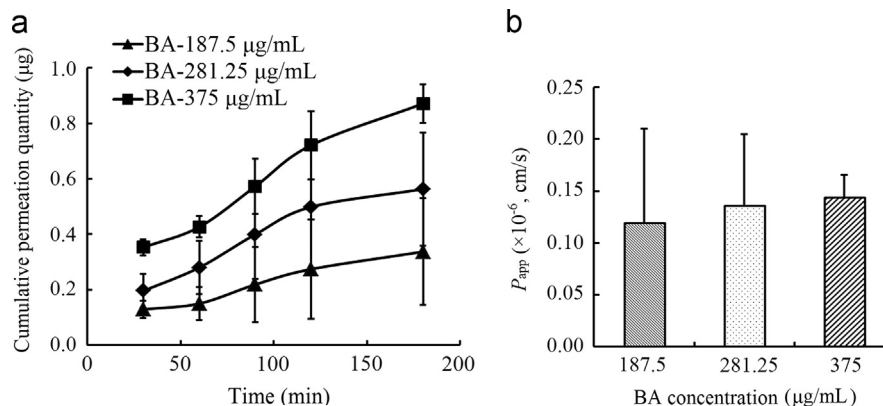
[*]$P<0.05$ compared with BA.

Figure 4   Cumulative permeation quantity (a) and apparent permeability coefficients (b) of BA through a Caco-2 monolayer at different concentrations. Data were expressed as mean$\pm$SD ($n=3$).
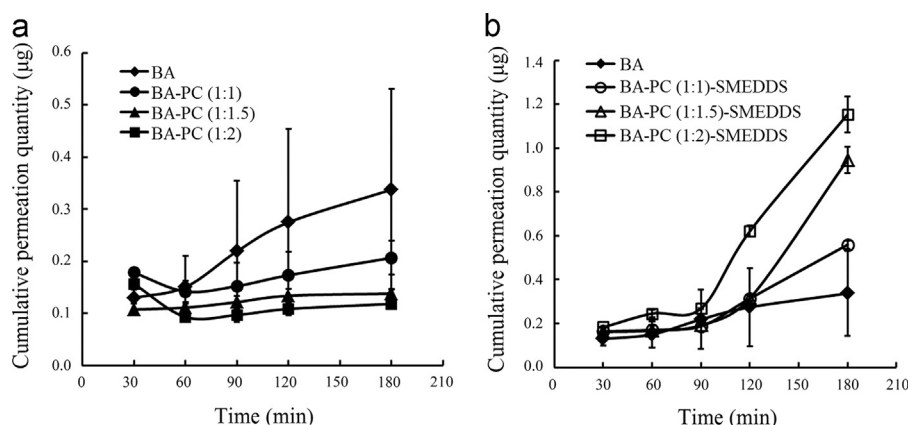

Figure 5   Comparison of cumulative permeation quantity (Q) through a Caco-2 monolayer between BA and BA–PC (a), BA and BA–PC–SMEDDS (b) at various molar ratios of drug to PP. Data were expressed as mean$\pm$SD ($n=3$).

48-fold in octanol when molar ratio of BA to PP was 1:1. Too high lipophilicity reduced the dispersion uniformity of BA–PC in buffer because of the special structure[51] (shown in Fig. 6) of PP. When the polar groups of PP such as positive choline group or negative phosphate group bond with the polar group of the drug by hydrogen bonds to form complex, the charges of PC were neutralized and entrapped easily by two lipophilic tails of PP. The comparison of P_{app} between BA and BA–PC demonstrates that appropriate balance between lipophilicity and hydrophilicity is very important for biomembrane transport.

The disadvantage of PC was remedied by the use of SMEDDS which facilitated a better dispersibility of BA–PC–SMEDDS in buffer. The Q and P_{app} of BA–PC–SMEDDS were significantly higher than that of BA (Figure 5b and Table 3) and increased with increasing molar ratio of BA to PP after 90 min. Since the toxicity of surfactant in SMEDDS was monitored by MTT and TEER and the data showed that the cell viability and integrity did not change significantly during the experiment (data not shown), the results presented in Fig. 5b and Table 3 show that the permeation of BA was markedly enhanced by PC–SMEDDS. In addition, SMEDDS itself can enhance the permeation of drugs. Thus, it also indicated that PC and SMEDDS had synergistic effects for improving the biomembrane transport of BA. The bioavailability of drug is greater than 1% but less than 100% in humans if the permeability coefficients are in the range of 0.1×10^{-6}–1.0×10^{-6} cm/s in Caco-2 cell[52], so BA–PC–SMEDDS, especially BA–PC(1:2)–SMEDDS ($P_{app} = (0.774 \pm 0.084) \times 10^{-6}$ cm/s) might have good oral absorption.
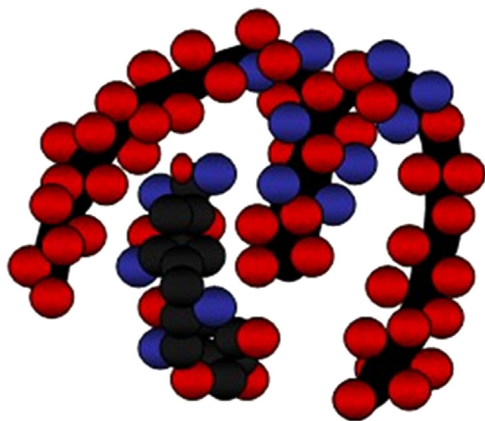
The reason why there was no significant difference of Q between BA and BA–PC–SMEDDS in the first 90 min ($P > 0.05$) might be explained in terms of the release of BA needed to overcome the intermolecular forces between BA and PP. Although Tween 80 in the BA–PC–SMEDDS formulation was a P-gp inhibitor, there might be less contact area between SMEDDS and the cells at first, resulting in BA, as the substrate of P-gp described above, showing an apparent increase in efflux in the first 90 min.

3.4. Single-pass intestinal perfusion

From the *in vitro* Caco-2 monolayer permeation study, we have demonstrated that BA–PC–SMEDDS could increase the P_{app} of BA. Since the SPIP approach in rats had been shown to be a precise method to predict *in vivo* oral absorption in man, this model was used to verify further the results from Caco-2 cells.

The data in Table 4 depicted the SPIS results of BA–PC and BA–PC–SMEDDS at lowest and highest molar ratios of BA to PP (*e.g.*, 1:1 and 1:2). The P_{eff} of BA in colon was significantly ($P < 0.05$) higher than in the other intestinal segments, followed by the ileum and upper intestinal site (including duodenum and jejunum). The highest P_{eff} of BA in the colon suggested that colon was the main absorption site, and did not change with the formation of BA–PC and BA–PC–SMEDDS. The P_{eff} of BA–PC and BA–PC–SMEDDS had the same tendency

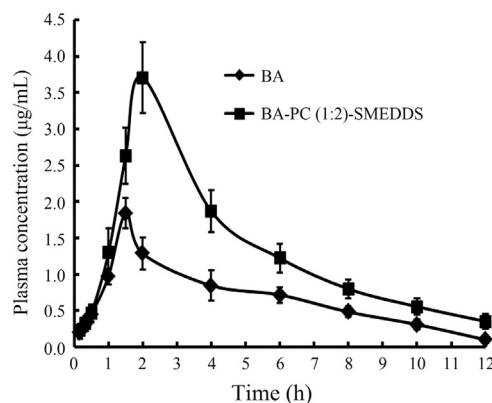**Figure 6** Schematic diagram of PC.

Figure 7 Plasma concentration–time profiles of BA in rats after oral administration BA and BA–PC(1:2)–SMEDDS. Data were expressed as mean $\pm$ SD ($n=6$).

Table 4 Effects of BA–PC and BA–PC–SMEDDS at different molar ratios on effective permeability coefficients (P_{eff}) of BA in different intestine segments.

Formulation	BA:PP	P_{eff} ($\times 10^{-4}$, cm/s)[a]		
		Duodenum+jejunum	Ileum	Colon
BA	–	0.139 ± 0.035*	0.252 ± 0.081*	0.506 ± 0.088
BA–PC	1:1	0.078 ± 0.021*,#	0.152 ± 0.033*	0.504 ± 0.075
	1:2	0.129 ± 0.019*	0.297 ± 0.054*	0.456 ± 0.033
BA–PC–SMEDDS	1:1	0.159 ± 0.034*	0.583 ± 0.099*,#	1.459 ± 0.235#
	1:2	0.513 ± 0.040*,#	1.173 ± 0.119*,#	2.229 ± 0.284#

[a]Data were expressed as mean $\pm$ SD, $n=6$.
*$P < 0.05$ compared to colon.
#$P < 0.05$ compared to BA.

Table 5 Pharmacokinetic parameters in rats after oral administration of BA and BA–PC(1:2)–SMEDDS.

Formulation	T_{max} (h)	C_{max} (μg/mL)	AUC (μg · h/mL)	F_r (%)
BA	1.5 ± 0.0	1.84 ± 0.47	7.61 ± 1.58	220.37 ± 49.93
BA–PC(1:2)–SMEDDS	2.0 ± 0.0[*]	3.74 ± 1.15[**]	17.28 ± 3.62[**]	

Data were presented as mean $\pm$ SD, $n=6$.
[*]$P<0.05$ compared to BA group.
[**]$P<0.01$ compared to BA group.

with Caco-2 cells, *i.e.*, PC did not facilitate the permeation of BA, but the permeation of BA could be enhanced significantly by PC–SMEDDS. The P_{eff} of BA–PC–SMEDDS increased noticeably in all the segments except BA–PC(1:1)–SMEDDS in duodenum and jejunum (non-main absorption site) ($P<0.05$), compared to that of free BA. Moreover, when the $P_{eff} > 0.42 \times 10^{-4}$ cm/s[53,54], the drug could be considered well absorbed in human. Therefore, the permeation improvement of BA formulated in PC(1:2)–SMEDDS was demonstrated further by SPIS.

3.5. Relative oral bioavailability of BA–PC–SMEDDS and BA suspensions

Taking into consideration of the results from Caco-2 cells and SPIS, BA–PC(1:2)–SMEDDS, as the optimal formulation, was used for the oral bioavailability study *in vivo* and the BA suspension at the same dose was used to evaluate bioavailability. Fig. 7 shows the plasma concentration–time profiles obtained after administration of BA suspension and BA–PC(1:2)–SMEDDS. The pharmacokinetic parameters are shown in Table 5. Significant differences were found for C_{max}, T_{max} and AUC. The C_{max} and AUC of PC–SMEDDS group were remarkably bigger than those of free BA group ($P<0.01$), and relative bioavailability (F_r) was $220.37 \pm 49.93\%$. The results suggested that PC–SMEDDS increased significantly the oral absorption of BA in rats. T_{max} of free BA group was smaller than that of BA–PC(1:2)–SMEDDS group ($P<0.01$) and might be due to the delayed release of BA from BA–PC–SMEDDS.

Base on the results above, the present research indicated that the combination of PC and SMEDDS could improve simultaneously the solubility in aqueous medium and biomembrane permeation of BA *in vitro* as determined from the physical and chemical models, Caco-2 cells, and SPIS, and the increased oral absorption of BA from the optimal dosage form of PC–SMEDDS was demonstrated in the rat *in vivo* model, which was consistent with *in vitro* studies. Therefore, the *in vitro* model study is very important for druggability research, especially given the issues of animal ethics, cost, time and huge candidate compounds. From the *in vitro* model, the optimal dosage form of a drug can be designed and verified *in vivo*.

4. Conclusions

The synergistic effects of PC and SMEDDS on enhancing the bioavailability of BA, a BCS class IV compound, have been studied systematically by *in vitro* physical and chemical models, a Caco-2 cell transport model, an *in situ* SPIP model and *in vivo* rat model. Our results may be of important reference value for the oral

absorption of other class IV compound. PC–SMEDDS has a good balance for lipophilicity and hydrophilicity of drugs which is critical for oral absorption. Moreover, it is worth noticing that PC–SMEDDS cannot solve the oral absorption problems associated with all BCS IV drug. Drugs with a phenolic hydroxyl group should have a high complexation percentage with PC and good oral absorption by means of PC–SMEDDS based on the results of our studies. The correlation between the structure of a drug and complexation with PC will be reported in the future.

References

1. Xu J, Huang R, Yang YJ, Jin SJ, Zhang JF. Effects of baicalin on apoptosis in rats with autoimmune encephalomyelitis. *Chin J Contemp Pediatr* 2011;**13**:665–8.
2. Kim SJ, Lee SM. Effect of baicalin on toll-like receptor 4-mediated ischemia/reperfusion inflammatory responses in alcoholic fatty liver condition. *Toxicol Appl Pharmacol* 2012;**258**:43–50.
3. Dou YQ, Du WL, Xue Y, Chen HZ, Zhao ML. Study on anti-endotoxin of baicalin. *West China J Stomatol* 2007;**25**:169–72.
4. Sahebkar A. Baicalin as a potentially promising drug for the management of sulfur mustard induced cutaneous complications: a review of molecular mechanisms. *Cutan Ocul Toxicol* 2011;**31**:226–34.
5. Novy P, Urban J, Leuner O, Vadlejch J, Kokoska L. *In vitro* synergistic effects of baicalin with oxytetracycline and tetracycline against *Staphylococcus aureus*. *J Antimicrob Chemother* 2011;**66**:1298–300.
6. Waisundara VY, Siu SY, Hsu A, Huang DJ, Tan BKH. Baicalin upregulates the genetic expression of antioxidant enzymes in Type-2 diabetic Goto–Kakizaki rats. *Life Sci* 2011;**88**:1016–25.
7. Woo AY, Cheng CHK, Waye MMY. Baicalein protects rat cardiomyocytes from hypoxia/reoxygenation damage *via* a prooxidant mechanism. *Cardiovasc Res* 2005;**65**:244–53.
8. Takahashi H, Chen MC, Pham H, Angst E, King JC, Park J, et al. Baicalein, a component of Scutellaria baicalensis, induces apoptosis by Mcl-1 down-regulation in human pancreatic cancer cells. *Biochim Biophys Acta* 2011;**1813**:1465–74.

9. Yang J, Yang X, Chu YW, Li M. Identification of baicalin as an immunoregulatory compound by controlling T(H)17 cell differentiation. *PLoS One* 2011;**6**:1–10.

10. Du GJ, Han G, Zhang S, Lin HH, Wu XC, Wang M, et al. Baicalin suppresses lung carcinoma and lung metastasis by SOD mimic and HIF-1alpha inhibition. *Eur J Pharmacol* 2010;**630**:121–30.

11. Li WM. New therapeutic aspects of flavones: the anticancer properties of Scutellaria and its main active constituents wogonin, baicalein and baicalin. *Cancer Treat Rev* 2009;**35**:57–68.

12. Ma AT, Zhong XH, Meng LG, Du J, Xu L. The overview of Skullcap flavone pharmacological research. *Chin J Vet Sci* 2006;**24**:39–40.

13. Zhang HH, Jiao QW, Gong QF, Zhang Y, Zhang WD, Hu ZL. Baicalin induced dendritic cell apoptosis *in vitro*. *Front Pharmacol* 2011;**2**:15.

14. Gong MT, Yu LF, Chen QH. The pharmacokinetics research in Baiclin andBaicelein orally taken by rats. *Chin Tradit Herb Drugs* 2009;**40**:392–4. (in Chinese).

15. Wang J, Ling HQ, Li ZG, Zhang XD. Preparation and dissolution determination of bacialin solid dispersion. *Chin J Exp Tradit Med Form* 2010;**16**:23–4.

16. Cui MY, Wang Y, Sun ZW, Ma YL, Li XN. Preparation and *in vitro* evaluation of baicalin microcapsule. *Chin J Exp Tradit Med Form* 2011;**17**:33–5.

17. Wang YM, Yue HK, Chang M, Zhang J, Qi L. Study on the preparation of bacialin sustain-release microcapsule. *J Anhui Agri Sci* 2011;**39**:12086–8.

18. Jia JP, Xing J, Qin XM, Cai LQ. Preparation and dissolution determination of inclusion compound capsule of baicalin with *β*-CD. *Chin J Drug Appl Monit* 2009;**6**:274–6.

19. Luo XQ, Yang JQ. Prescription design and dissolution evaluation of self-emulsifying drug delivery systems of baicalin. *J Chin Med Mater* 2010;**33**:1157–9.

20. Li N, Je YJ, Yang M, Jiang XH, Ma JH. Pharmacokinetics of baicalin-phospholipid complex in rat plasma and brain tissues after intranasal and intravenous administration. *Pharmamzie* 2011;**66**:374–7.

21. Gabrielska J, Oszmiański J, Zyłka R, Komorowska M. Antioxidant activity of flavones from Scutellariabaicalensis in lecithin liposomes. *Z Naturforsch C* 1997;**52**:817–23.

22. Liu ZD, Zhang XH, Wu HY, Li JW, Shu LX, Liu R, et al. Preparation and evaluation of solid lipid nanoparticles of baicalin for ocular drug delivery system *in vitro* and *in vivo*. *Drug Dev Ind Pharm* 2011;**37**:475–81.

23. Sindhumol PG, Maria T, Mohanachandran PS. A novel dosage form for enhancement of bioavailability of botanicals and neutraceuticals. *Int J Pharm Sci* 2010;**2**:104.

24. Nilesh J, Brahma PG, Navneet T, Ruchi J, Jitendra B, Deepak KJ, et al. Phytosome: a novel drug delivery system for herbal medicine. *Int J Pharm Sci Drug Res* 2010;**2**:224–8.

25. Qin X, Yang Y, Fan TT, Gong T, Zhang XN, Huang Y. Preparation, characterization and *in vivo* evaluation of bergenin–phospholipid complex. *Acta Pharmacol Sin* 2010;**31**:127–36.

26. Maiti K, Mukherjee K, Gantait A, Saha BP, Mukherjee PK. Curcumin–phospholipid complex: preparation, therapeutic evaluation and pharmacokinetic study in rats. *Int J Pharm* 2007;**330**:155–63.

27. Xiao YY, Song YM, Chen ZP, Ping QN. The preparation of silybin–phospholipid complex and the study on its pharmacokinetics in rats. *Int J Pharm* 2006;**307**:77–82.

28. Constantinides PP. Lipid microemulsions for improving drug dissolution and oral absorption: physical and biopharmaceutical aspects. *Pharm Res* 1995;**12**:1561–72.

29. Constantinides PP, Scalart J. Formulation and physical characterization of water-in-oil microemulsions containing long- *versus* medium-chain glycerides. *Int J Pharm* 1997;**158**:57–68.

30. Singh AK, Chaurasiya A, Singh M, Upadhyay SC, Mukherjee R, Khar RK. Exemestane loaded self-microemulsifying drug delivery system (SMEDDS):development and optimization. *AAPS Pharm Sci Tech* 2008;**9**:628–34.

31. Patel AR, Vavia PR. Preparation and *in vivo* evaluation of SMEDDS (self-microemulsifying drug delivery system) containing fenofibrate. *AAPS J* 2007;**9**:344–52.

32. Gursoy RN, Benita S. Self-emulsifying drug delivery systems (SEDDS) for improved oral delivery of lipophilic drugs. *Biomed Pharmacother* 2004;**58**:173–82.

33. Li XR, Yuan Q, Huang YQ, Zhou YX, Liu Y. Development of silymarin self-microemulsifying drug delivery system with enhanced oral bioavailability. *AAPS Pharm Sci Tech* 2010;**11**:672–8.

34. Zhang P, Liu Y, Feng NP, Xu J. Preparation and evaluation of self-microemulsifying drug delivery system of oridonin. *Int J Pharm* 2008;**355**:269–76.

35. Setthacheewakul S, Mahattanadul S, Phadoongsombut N, Pichayakorn W, Wiwattanapatapee R. Development and evaluation of self-microemulsifying liquid and pellet formulations of curcumin and absorption studies in rats. *Eur J Pharm Biopharm* 2010;**76**:475–85.

36. Yue PF, Yuan HL, Li XY, Yang M, Zhu WF. Process optimization, characterization and evaluation *in vivo* of oxymatrine–phospholipid complex. *Int J Pharm* 2010;**387**:139–46.

37. Miller JM, Dahan A, Gupta D, Varghese S, Amidon GL. Enabling the intestinal absorption of highly polar antiviral agents: in-pair facilitated membrane permeation of zanamivir heptyl ester and guanidino oseltamivir. *Mol Pharm* 2010;**7**:1223–34.

38. Engelmann FM, Rocha SVO, Toma HE, Araki K, Baptista MS. Determination of *n*-octanol/water partition and membrane binding of cationic porphyrins. *Int J Pharm* 2007;**329**:12–8.

39. Kobayashi S, Tanabe S, Sugiyama M, Konishi Y. Transepithelial transport of hesperetin and hesperidin in intestinal Caco-2 cell monolayers. *Biochim Biophys Acta* 2008;**1778**:33–41.

40. Kobayashi S, Konishi Y. Transepithelial transport of flavanone in intestinal Caco-2 cell monolayers. *Biochem Biophys Res Commun* 2008;**368**:23–9.

41. Farrell TL, Poquet L, Dew TP, Barber S, Williamson G. Predicting phenolic acid absorption in Caco-2 cells: a theoretical permeability model and mechanistic study. *Drug Metab Dispos* 2012;**40**:397–406.

42. Zakeri-Milani P, Valizadeh H, Tajerzadeh H, Azarmi Y, Islambolchilar Z, Barzegar S, et al. Predicting human intestinal permeability using single-pass intestinal perfusion in rat. *J Pharm Pharm Sci* 2007;**10**:368–79.

43. Cummins CL, Salphati L, Reid MJ, Benet LZ. *In vivo* modulation of intestinal CYP3A metabolism by p-Glycoprotein: studies using the rat single-pass intestinal perfusion model. *J Pharmacol Exp Ther* 2003;**305**:306–14.

44. Zhang L, Lin G, Chang Q, Zuo Z. Role of intestinal first-pass metabolism of baicalein in its absorption process. *Pharm Res* 2005;**22**:1050–8.

45. Crowe A, Lemaire M. *In vitro* and *in situ* absorption of SDZ-RAD using a human intestinal cell line (Caco-2) and a single pass perfusion model in rats: comparison with rapamycin. *Pharm Res* 1998;**5**:1666–72.

46. Sutton SC, Rinaldi MT, Vukovinsky KE. Comparison of the gravi-metric, phenol red, and 14C-PEG-3350 methods to determine water absorption in the rat single-pass intestinal perfusion model. *AAPS Pharm Sci* 2001;**3**:E25.

47. Balakrishnan P, Lee BJ, Oh DH, Kim JO, Lee YI, Kim DD, et al. Enhanced oral bioavailability of coenzyme Q10 by self-emulsifying drug delivery systems. *Int J Pharm* 2009;**374**:66–72.

48. Abraham DJ. *Burger's medicinal chemistry and drug discovery. Vol. 2: drug discovery and drug development*. New Zealand: John Wiley & Sons Inc; 2003, p. 249–93.

49. Sha XY, Yan GJ, Wu YJ, Li JC, Fang CL. Effect of self-microemulsifying drug delivery systems containing Labrasol on tight junctions in Caco-2 cells. *Eur J Pharm Sci* 2005;**24**:477–86.

50. Nerurkar MM, Burton PS, Borchardt RT. The use of surfactants to enhance the permeability of peptides through Caco-2 cells by inhibition of an apically polarized efflux system. *Pharm Res* 1996;**13**:528–34.

51. Semalty A, Semalty M, Rawat MSM, Franceschi F. Supramolecular phospholipids–polyphenolics interactions: the phytosome strategy to

improve the bioavailability of phytochemicals. *Fitoterapia* 2010;**81**:306–14.

52. Artursson P, Karlsson J. Correlation between oral drug absorption in humans and apparent drug permeability coefficients in human intestinal epithelial (Caco-2) cells. *Biochem Biophys Res Commun* 1991;**175**:880–5.

53. Fagerholm U, Johansson M, Lennernäs H. Comparison between permeability coefficients in rat and human jejunum. *Pharm Res* 1996;**13**:1336–42.

54. Amidon GL, Sinko PJ, Fleisher D. Estimating human oral fraction dose absorbed: a correlation using rat intestinal membrane permeability for passive and carrier-mediated compounds. *Pharm Res* 1988;**5**:651–4.